ACS APPLIED MATERIALS & INTERFACES

Research Article

www.acsami.org

A Universal Electron-Transporting/Exciton-Blocking Material for Blue, Green, and Red Phosphorescent Organic Light-Emitting Diodes (OLEDs)

Cheng-Hung Shih, Pachaiyappan Rajamalli, Cheng-An Wu, Wei-Ting Hsieh, and Chien-Hong Cheng*

Department of Chemistry, National Tsing Hua University, Hsinchu 30013, Taiwan

Supporting Information

ABSTRACT: Three *m*-terphenyl oxadiazole derivatives, 3,3″-bis(5-(pyridin-4-yl)-1,3,4-oxadiazol-2-yl)-1,1′:3′,1″-terphenyl (4PyOXD), 3,3″-bis(5-(pyridin-3-yl)-1,3,4-oxadiazol-2-yl)-1,1′:3′,1″-terphenyl (3PyOXD), and 3,3″-bis(5-phenyl-1,3,4-oxadiazol-2-yl)-1,1′:3′,1″-terphenyl (PhOXD), were synthesized. They exhibit relatively high electron mobilities compared with those of known electron-transport materials such as TAZ, BAlq, and BCP+Alq_3. These materials were then utilized as electron transporters and hole/exciton blockers for blue, green, and red phosphorescent organic light-emitting diodes. The devices exhibited reduced driving voltages, very high efficiency, and negligible roll-off. More importantly, among these three oxadiazole derivatives, PhOXD performed as an ideal electron-transporting material for the blue, green, and red devices with excellent external quantum efficiencies (EQEs, >26%) as well as current and power efficiencies. Using these materials as an electron-transporting/exciton-blocking layer, low roll-off was achieved for the devices, indicative of excellent confinement of the triplet excitons in the emitting layer even at high current densities. At the normal operation brightness of 1000 cd m^{-2}, the EQEs remained >21.3% for these basic color devices. In addition, the relationships between physical properties and structures of the molecules such as the electron mobility, triplet energy gap, and efficiency can be clearly rationalized.

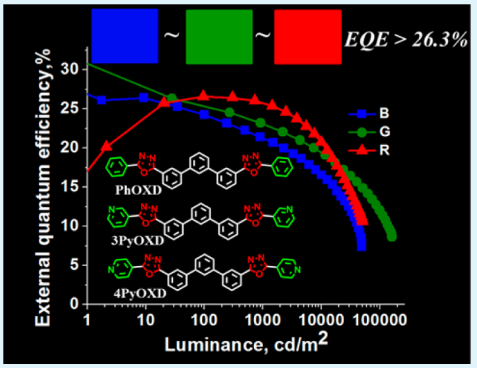

KEYWORDS: *electron-transport material, improved roll-off, phosphorescent OLED, universal, oxadiazole*

INTRODUCTION

Organic light-emitting diodes (OLEDs) have drawn a great deal of attention because of their outstanding performance in display technology and lighting.[1−10] High-efficiency OLEDs with a low driving voltage and simplified device structure are very important for their commercial application. Phosphorescence organic light-emitting devices (PhOLEDs) are the best option because their external/internal quantum efficiencies are 4 times as high as those of conventional fluorescence-based OLEDs, by harvesting both singlet and triplet excitons.[11−19] Recombination of holes and electrons within the emitting layer results in the generation of illumination in OLEDs. Consequently, the efficiency of an OLED depends greatly upon the effective recombination of holes and electrons in the emitting layer (EML).[20−23] In the design of an exceptionally high-efficiency phosphorescent device, the appropriate selection of materials for each layer is also essential. In particular, electron-transport materials with high electron mobility and proper singlet and triplet energy gaps are in high demand because it is known that the electron mobilities of organic materials are mostly much lower than the hole mobilities.[24]

In general, because of the long lifetime, the triplet exciton of an EML material (dopant or host) exhibits a long diffusion length to the adjacent layers compared with that of the singlet exciton.[25,26] Therefore, it is important that the electron-transport material (ETM) have a large enough triplet energy gap (E_T) to prevent diffusion of the triplet exciton from the EML to the electron-transporting layer (ETL). It is a big challenge to design and synthesize an ETM with sufficient E_T, high electron mobility, and high thermal stability that can be used in the ETL, particularly for the blue phosphorescence OLEDs. Unfortunately, it is quite difficult to meet the demand because there is a trade-off between the material energy gap and mobility and thermal stability.[27,28] There are many electron-transport materials that have been developed to improve the efficiency of PhOLEDs,[29−35] but most of these materials exhibit significant roll-off of the devices. While some of these materials are particularly suitable for a single-color device, none of them has been used as a universal ETM.[36−39] To fabricate a RGB full-color OLED display, a large number of materials are required if different materials are used by blue, green, and red devices. However, the manufacturing cost will be tremendously reduced if some of the materials can be shared with different color devices to reduce the number of materials and thus the

Received: March 2, 2015
Accepted: April 15, 2015
Published: April 15, 2015

DOI: 10.1021/acsami.5b01872
ACS Appl. Mater. Interfaces 2015, 7, 10466−10474

Scheme 1. Synthetic Route for the *m*-Terphenyl Oxadiazole Derivatives

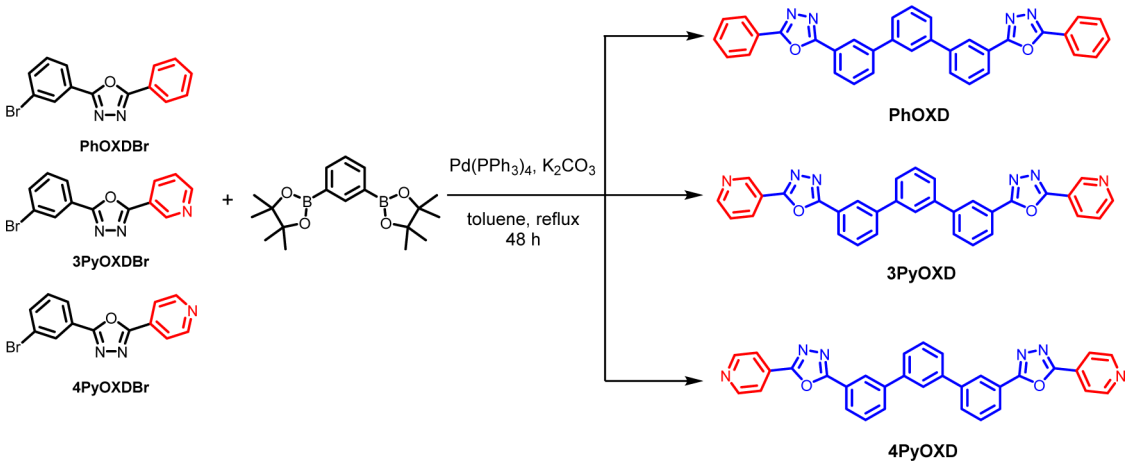

equipment needed to fabricate the OLED display. Hence, there is a great demand for designing a universal ETM for all color OLEDs to reduce the manufacturing expenses. Recently, we reported several oxadiazole-based thermally stable electron-transport materials for RGB devices with high EQEs and power efficiencies.[30,40] In this report, we designed and synthesized three new *m*-terphenyl oxadiazole derivatives, 4PyOXD, 3PyOXD, and PhOXD (Scheme 1), for use as electron-transporting/exciton-blocking materials for blue, green, and red OLEDs. Surprisingly, all three RGB devices using PhOXD for the ETL exhibit extremely high device efficiencies with EQEs of >26%. Their current and power efficiencies are also among the best ever reported. In addition, at the normal operation brightness of 1000 cd m^{-2}, the EQEs still remain >21.3% for the blue, green, and red devices.

EXPERIMENTAL SECTION

Physical property and OLED fabrication measurements were taken using the reported methods.[30,40]

Synthesis of 3″-Bis(5-phenyl-1,3,4-oxadiazol-2-yl)-1,1′:3′,1″-terphenyl (PhOXD). 2-(3-Bromophenyl)-5-phenyl-1,3,4-oxadiazole (PhOXDBr) (1.98 g, 6.60 mmol), 1,3-bis(4,4,5,5-tetramethyl-1,3,2-dioxaborolan-2-yl)benzene (1.0 g, 3.00 mmol), and $K_2CO_{3(aq)}$ (2 M, 30 mL) were placed in a double-necked flask and purged with nitrogen gas. Then $Pd(PPh_3)_4$ (346 mg, 0.30 mmol) and toluene (90 mL) were quickly added, and the reaction mixture was heated to reflux for 48 h. After completion of the reaction, the mixture was cooled to room temperature, the solution was filtered through a Celite pad, and to the filtered solution were added methylene chloride and water. After being vigorously shaken, the organic layer was separated from the aqueous layer. The aqueous phase was further extracted by methylene chloride once. The combined organic solution was dried with $MgSO_4$, concentrated under reduced pressure to remove the solvent, and then purified by a silica gel column using a mixture of ethyl acetate and *n*-hexane as the eluent (1:4) to give the expected white solid product in 85% yield: ^{1}H NMR (400 MHz, $CDCl_3$) δ 8.39 (s, 2H), 8.14−8.11 (m, 6H), 7.89 (s, 1H), 7.82 (d, J = 8 Hz, 2H), 7.67 (d, J = 8 Hz, 2H), 7.64−7.56 (m, 3H), 7.52−7.48 (m, 6H); ^{13}C NMR (100 MHz, $CDCl_3$) δ 164.68, 164.46, 141.92, 140.68, 131.75, 130.54, 129.65, 129.60, 129.06, 126.95, 126.84, 126.12, 125.91, 125.60, 124.50, 123.81; HRMS [M^+] calcd for $C_{34}H_{22}N_4O_2$ m/z 518.1743, found m/z 518.1744. Anal. Calcd for $C_{34}H_{22}N_4O_2$: C, 78.85; H, 4.80; N, 10.80; O, 6.17. Found: C, 78.32; H, 4.39; N, 10.83; O, 6.64.

Synthesis of 3,3″-Bis(5-(pyridin-3-yl)-1,3,4-oxadiazol-2-yl)-1,1′:3′,1″-terphenyl (3PyOXD). A procedure similar to the synthesis of PhOXD was used for the synthesis of 3PyOXD by the Suzuki coupling reaction of 1,3-bis(4,4,5,5-tetramethyl-1,3,2-dioxaborolan-2-yl)benzene with 2-(3-bromophenyl)-5-(pyridin-3-yl)-1,3,4-oxadiazole (3PyOXDBr) to give the desired product in 76% yield: ^{1}H NMR (400 MHz, $CDCl_3$) δ 9.35 (s, 2H), 8.76 (d, J = 4 Hz, 2H), 8.44−8.40 (m, 4H), 8.12 (d, J = 7.2 Hz, 2H), 7.89 (s, 1H), 7.85 (d, J = 7.6 Hz, 2H), 7.69−7.57 (m, 5H), 7.49−7.46 (m, 2H); ^{13}C NMR (100 MHz, $CDCl_3$) δ 164.99, 162.56, 152.41, 147.85, 141.92, 140.52, 134.12, 130.82, 129.74, 129.64, 126.85, 126.04, 125.99, 125.67, 124.05, 123.78, 120.32; HRMS [M+] calcd for $C_{32}H_{20}N_6O_2$ m/z 520.1648, found m/z 520.1654. Anal. Calcd for $C_{32}H_{20}N_6O_2$: C, 73.84; H, 3.87; N, 16.14; O, 6.15. Found: C, 73.69; H, 4.00; N, 15.87; O, 6.44.

Synthesis of 3,3″-Bis(5-(pyridin-4-yl)-1,3,4-oxadiazol-2-yl)-1,1′:3′,1″-terphenyl (4PyOXD). A procedure similar to the synthesis of PhOXD was also used for the synthesis of 4PyOXD by the Suzuki coupling of 1,3-bis(4,4,5,5-tetramethyl-1,3,2-dioxaborolan-2-yl)-benzene with 2-(3-bromophenyl)-5-(pyridin-4-yl)-1,3,4-oxadiazole (4PyOXDBr) to give 4PyOXD in 78% yield: ^{1}H NMR (400 MHz, $CDCl_3$) δ 8.82 (d, J = 5.6 Hz, 4H), 8.41 (s, 2H), 8.12 (d, J = 7.6 Hz, 2H), 7.99−7.97 (m, 4H), 7.89−7.84 (m, 3H), 7.69−7.57 (m, 5H); ^{13}C NMR (100 MHz, $CDCl_3$) δ 165.34, 162.89, 150.90, 142.01, 140.53, 131.03, 130.87, 129.80, 129.69, 126.91, 126.10, 125.83, 125.75, 123.97, 120.30; HRMS [M^+] calcd for $C_{32}H_{20}N_6O_2$ m/z 520.1648, found m/z 520.1635. Anal. Calcd for $C_{32}H_{20}N_6O_2$: C, 73.84; H, 3.87; N, 16.14; O, 6.15. Found: C, 73.73; H, 3.89; N, 16.13; O, 6.25.

RESULTS AND DISCUSSION

The synthetic routes for PhOXD, 3PyOXD, and 4PyOXD are presented in Scheme 1. These materials were prepared by the Suzuki coupling reaction of 1,3-bis(4,4,5,5-tetramethyl-1,3,2-dioxaborolan-2-yl)benzene with the corresponding bromo compounds PhOXDBr, 3PyOXDBr, and 4PyOXDBr, respectively, in excellent yields. The products were further purified by sublimation and characterized by ^{1}H NMR, ^{13}C NMR, high-resolution mass spectrometry, and elemental analysis. The detailed synthesis procedure is provided in the Experimental Section, and the characterization data are presented in the Supporting Information.

The core structure of these three materials consists of an *m*-terphenyl and two oxadiazole moieties. The three phenylenes of the *m*-terphenyl component are connected to other components through the *meta* positions. This arrangement is expected to provide the molecules with high glass transition temperatures (T_gs) and high triplet energy gaps (E_Ts) because of the limited conjugation between the *m*-phenylene rings.[6] Oxadiazole is known to be a high-electron affinity component for ETMs with high electron mobility. In addition, it exhibits a wide triplet energy gap property because of the restricted π-conjugation beyond the ring, although the molecule is coplanar. These *meta* terphenyl oxadiazole materials were tested as

DOI: 10.1021/acsami.5b01872
ACS Appl. Mater. Interfaces 2015, 7, 10466−10474

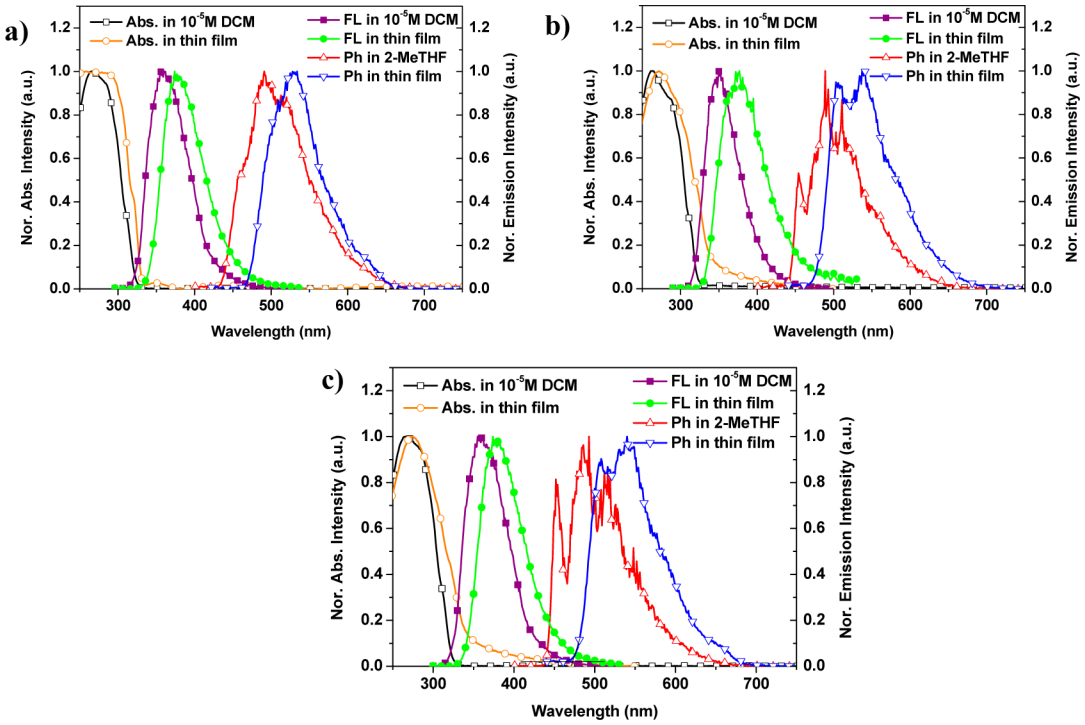

Figure 1. Absorption (Abs.), fluorescence (FL.), and phosphorescence (Ph.) spectra of (a) PhOXD, (b) 3PyOXD, and (c) 4PyOXD. The Abs. and FL spectra were measured at room temperature, and the Ph. spectra were measured at 77 K.

Table 1. Physical and Thermal Properties of PhOXD, 3PyOXD, and 4PyOXD

materials	λ_{abs} (nm)[a]	$\lambda_{max,em}$ (nm)[a]	$\lambda_{max,em}$ (nm)[b]	HOMO/LUMO[c]	E_S/E_T[d](ev)	T_g/T_d (°C)	ref
PhOXD	280	374	493	5.84/2.25	3.59/2.70	83/444	this work
3PyOXD	273	377	503	5.90/2.30	3.60/2.65	93/445	this work
4PyOXD	273	374	508	5.95/2.36	3.59/2.62	104/448	this work
tOXD-*m*TP	252	347	494	6.05/2.19	3.86/2.83	63/344	30

[a]Measured in thin films. [b]The phosphorescences were measured in thin films at 77 K. [c]The LUMO levels were measured from the $E_{1/2re}$, and the HOMO levels were determined from LUMO + E_S. [d]The singlet energy gap (E_S) was determined from the wavelength of the intersection point of absorption and fluorescence spectra in the thin film, and E_T was determined from the onset of phosphorescence spectra in the thin film. T_g is the glass transition temperature; T_d is the decomposition temperature.

electron-transporting and exciton-blocking materials for iridium-based blue, green, and red phosphorescent OLEDs.

Physical Properties. The UV−vis absorption, photoluminescence, and phosphorescence spectra of PhOXD, 3PyOXD, and 4PyOXD were measured in dichloromethane solutions and thin films at room temperature and 77 K, as observed in Figure 1, and the key spectral and thermal properties data are summarized in Table 1. All the compounds exhibit an absorption band at approximately 260−270 nm in a dichloromethane solution, which may be assigned to the $\pi-\pi^*$ transition of the oxadiazole moiety.[41] Fluorescent emission peaks for PhOXD, 3PyOXD, and 4PyOXD in dichloromethane solutions appear at 362, 351, and 362 nm, respectively. The thin film fluorescent and phosphorescence emission peaks were observed at 374 and 493 nm for PhOXD, 377 and 503 nm for 3PyOXD, and 374 and 508 nm for 4PyOXD, respectively. The photoluminescence peak is approximately red-shifted by 15 nm in the solid thin film related to the solution likely because of the intermolecular $\pi-\pi$ interaction in the thin film. The electrochemical properties of these compounds were measured using cyclic voltammetry (CV), and the curves are presented in Figure S1 of the Supporting Information.

The energy gaps (E_g) of PhOXD, 3PyOXD, and 4PyOXD are 3.59, 3.60, and 3.59 eV, respectively. The E_gs were calculated from the intersection of the absorption and emission spectra of the molecules. The HOMO and LUMO levels were calculated to be 5.84 and 2.25 eV for PhOXD, 5.90 and 2.30 eV for 3PyOXD, and 5.95 and 2.36 eV for 4PyOXD, respectively. The LUMO levels were measured from reduction potentials $E_{1/2re}$, and the HOMO levels were determined from LUMO + E_S. The triplet energy gaps (E_T) of these materials were calculated to be 2.70, 2.65, and 2.62 eV for PhOXD, 3PyOXD, and 4PyOXD, respectively. E_Ts were calculated from the onset of phosphorescence spectra in the thin film at 77 K. The E_Ts of these electron-transporting materials are higher than those of conventional ETL materials such as tris(8-hydroxyquinolinato) aluminum (Alq_3) (E_T = 2.0 eV) and bis(8-hydroxy-2-methylquinoline)-(4-phenylphenoxy)aluminum (BAlq) (E_T = 2.2 eV). The electronic properties of these materials vary because of the presence of different functional groups at the terminal positions of the molecules. The HOMO and LUMO levels decrease systematically in the following order: PhOXD > 3PyOXD > 4PyOXD. The E_Ts decrease in the following order: PhOXD > 3PyOXD > 4PyOXD. The E_T of PhOXD is higher than that of the blue iridium complex dopant, suggesting that

DOI: 10.1021/acsami.5b01872
ACS Appl. Mater. Interfaces 2015, 7, 10466−10474

the triplet excitons are well confined within the EML when PhOXD served as an ETL/EBL. In addition, these oxadiazole derivatives appear to possess deep HOMO levels to block the holes/exciton and appropriate LUMO levels for smooth electron injection.

The thermal properties were determined using thermogravimetric analysis (TGA) and differential scanning calorimetry (DSC) to understand the thermal stabilities of these electron-transporting materials, and the data are presented in Table 1 and Figures S2−S5 of the Supporting Information. Note that all these *m*-terphenyl oxadiazole derivatives exhibit high glass transition temperatures (T_gs) and high decomposition temperatures (T_d), indicative of the high stability of the deposited films. T_g and T_d increase when a pyridine ring is introduced into the material. Additionally, as the nitrogen atom position in the pyridine ring changes from 3 to 4, T_g and T_d further increase. This trend can be attributed to the increased level of intermolecular interaction of the nitrogen atom accompanied by the change in position from 3 to 4.[32]

To know the electron-transporting properties of these materials, electron-only devices were fabricated. The devices were fabricated using the following structure: ITO/BCP (15 nm)/ETM (40 nm)/LiF (1 nm)/Al (100 nm), where BCP is the 2,9-dimethyl-4,7-diphenyl-1,10-phenanthroline, and the current density versus voltage curves of these devices are presented in Figure 2. All these oxadiazole-based materials

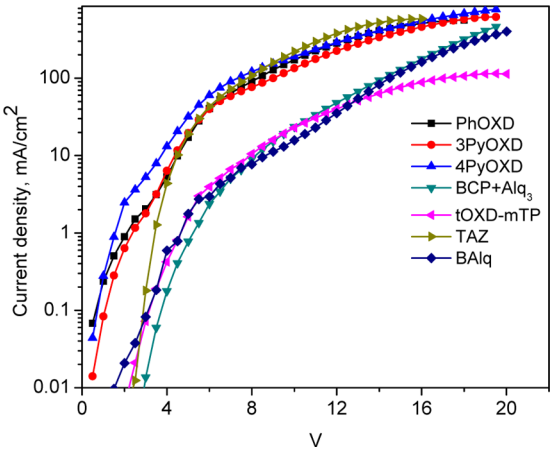

Figure 2. Current density vs voltage characteristics of the electron-only devices.

exhibit good electron mobility compared with that of the known ET materials such as Alq_3+BCP, BAlq, bis(2-*tert*-butyl-1,3,4-oxadiazole-5-diyl)-3,30-*m*-terphenyl (tOXD-*m*TP), and 3-(4-biphenyl)-4-phenyl-5-(4-*tert*-butylphenyl)-1,2,4-triazole (TAZ). Figure 2 shows that the current density at the same applied voltage of the electron-only devices follows the order 4PyOXD > 3PyOXD > PhOXD > TAZ > tOXD-*m*TP > BAlq > BCP+Alq_3 at low voltage. This result also indicates that when the phenyl ring (PhOXD) is replaced by the pyridine ring (3PyOXD or 4PyOXD), the electron mobility of the electron-only device increased. Furthermore, as the nitrogen atom position of pyridine ring changes from 3 to 4, the electron mobility increases further. This is because the intermolecular hydrogen bond is stronger for 4PyOXD.[32] Therefore, the position of the nitrogen atom in the pyridine appears to greatly affect the electron-transporting properties. In addition, electron mobilities of these materials were determined by the space charge-limited current (SCLC) method.[42,43] As shown in Figure S6 of the Supporting Information, the electron mobilities of PhOXD, 3PyOXD, and 4PyOXD are 4.2×10^{-6}, 1.2×10^{-5}, and 1.6×10^{-5} cm^2 V^{-1} s^{-1}, respectively. The results suggest that these materials have high electron mobilities in agreement with the trend of electron-only devices.

Device Performance. To assess the performance of PhOXD, 3PyOXD, and 4PyOXD as the ETL/EBL, several devices were fabricated using commercially available phosphorescent emitters. Devices B1−B3 using FIrpic as the dopant with a common device structure ITO/NPB (30 nm)/*m*CP (10 nm)/BCPO: FIrpic (8%) (30 nm)/ETL (40 nm)/LiF (1 nm)/Al (100 nm) were fabricated without using an exciton/hole-blocking layer between the EML and ETL. The ETLs of these devices were PhOXD, 3PyOXD, and 4PyOXD for B1−B3, respectively. In these devices, NPB [*N*,*N*′-bis(1-naphthyl)-*N*,*N*′-diphenyl-1,10-biphenyl-4,4′-diamine] acts as a hole-transporting material (HTL), *m*CP [1,3-bis(*N*-carbazolyl)benzene] acts as a hole-transporting material as well as an exciton blocker, and BCPO {bis-4-[(*N*-carbazolyl)phenyl]-phenylphosphine oxide} acts as a bipolar host material. The device architecture is illustrated in Figure 3.

Figure 4 presents the current density and luminance versus applied voltage plots of devices B1−B3, and the performance data are summarized in Table 2. Device B1 exhibits a turn-on voltage of 3.2 V (a luminance of 1 cd m^{-2} was detected), which is lower than the previously reported values for the device based on FIrpic as the dopant with conventional OXD-7 (3.9 V) and tOXD-*m*TP (3.9 V) as the ETL.[30] This finding is possibly due to the optimal LUMO level and high electron mobilities of PhOXD relative to those of the other layers in the device. In addition to the low turn-on voltage, an extremely high external quantum efficiency of 26.4%, a maximal brightness of 49600 cd m^{-2}, a current efficiency of 55.0 cd A^{-1}, and a power efficiency of 48.8 lm W^{-1} were achieved. These values are much higher than those for the previously reported FIrpic-based devices using conventional electron-transporting materials such as OXD-7 (EQE, 11.4%; luminance, 13280 cd m^{-2}) and TAZ (EQE, 12.5%; luminance, 16540 cd m^{-2}), which is 2−3 times lower than those of device B1.[30,44] Even though TAZ has a similar E_T gap, its molecular structure is not planar; therefore, the electron mobility is slow.[45] The electroluminescence spectra of this device are similar to that of a previously reported FIrpic-based device with comparable Commission Internationale de l'Éclairage (CIE) coordinates of (0.14, 0.32) (Figure S7 of the Supporting Information)[40] and no emission from adjacent materials. This result suggests that the recombination of the carriers (holes and electrons) occurs in the EML completely, and the excitons formed are well confined within the EML.

In general, phosphorescent OLEDs exhibit severe roll-off at a higher current density due to triplet−triplet annihilation.[46] The EQEs and current efficiencies versus the luminance of these devices are displayed in Figure S8 of the Supporting Information. In contrast to the previous reports,[47] this device exhibits low roll-off even at higher current density. At practical brightnesses of 100 and 1000 cd m^{-2}, the efficiency remains above 24.3 and 21.3%, respectively, without any light-outcoupling enhancement. Device B2 exhibits a turn-on voltage of 3.4 V, and device B3 exhibits the same turn-on voltage as device B1. The efficiencies of devices B2 and B3 are lower than those of B1: in fact only 5% EQE was observed for B3. This result is likely due to the unbalanced carriers or relatively low

DOI: 10.1021/acsami.5b01872
ACS Appl. Mater. Interfaces 2015, 7, 10466−10474

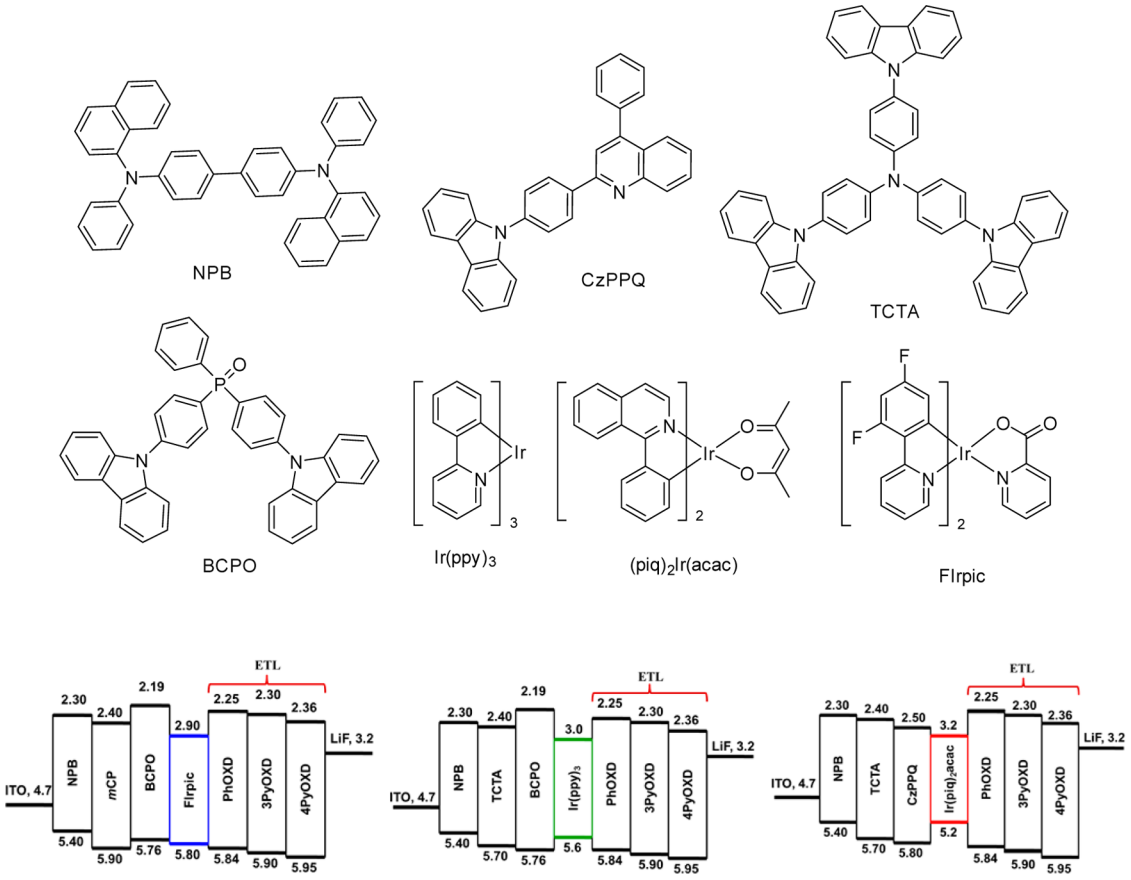

Figure 3. Structures of the organic materials used and the HOMO/LUMO levels for the materials used in the EL devices.

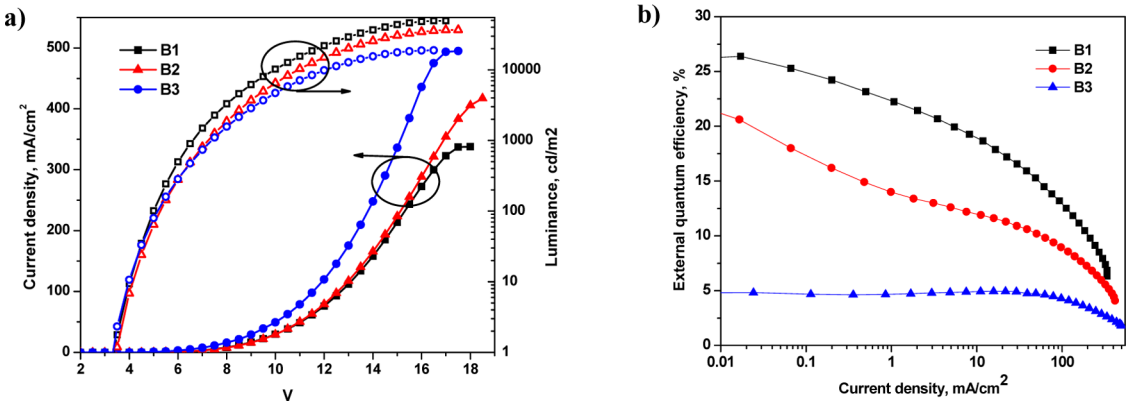

Figure 4. (a) Current density and luminance vs applied voltage and (b) external quantum efficiency vs current density of devices B1−B3. The device configuration is ITO/NPB (30 nm)/*m*CP (10 nm)/BCPO: FIrpic (8%) (30 nm)/PhOXD or 3PyOXD or 4PyOXD (40 nm)/LiF (1 nm)/Al (100 nm).

triplet energy levels of 3PyOXD and 4PyOXD, which may induce the exciton quenching by the diffusion of excitons from the emitting layer to the ETL. For device B3, a residual emission at approximately 407 nm was observed, indicating that there is exciton leakage (Figure S7 of the Supporting Information). PhOXD exhibits the highest efficiency and brightness among the three compounds; we speculate that PhOXD has enough E_T to confine excitons in the EML and a suitable LUMO level and high electron mobility to transfer electrons to the emitting layer.

In addition to the blue phosphorescent OLEDs, these oxadiazole-based electron-transporting materials, PhOXD, 3PyOXD, and 4PyOXD, were also utilized as an ETM for $Ir(ppy)_3$-based green devices. Three green light-emitting devices G1−G3 were fabricated using PhOXD, 3PyOXD, and 4PyOXD, respectively, as the ETL materials. The devices consist of the following layers: ITO/NPB (20 nm)/TCTA (10 nm)/BCPO: $Ir(ppy)_3$ (8%, 30 nm)/ETL (40 nm)/LiF (1 nm)/Al (100 nm). The voltage versus current density and luminance curves and the structures of the devices are shown in Figure 5. In these devices, TCTA was utilized as the exciton blocker to avoid exciton diffusion to the hole-transporting layer. It is noteworthy that TCTA is known to be an efficient exciton blocker for green phosphorescence devices.[48] Device G1 with

DOI: 10.1021/acsami.5b01872
ACS Appl. Mater. Interfaces 2015, 7, 10466−10474

Table 2. Electroluminescence Data for Devices B1−B3, G1−G3, and R1−R3[a]

device	ETM	V_d[b] (V)	L_{max} (cd m^{-2}, V)	EQE$_{max}$ (%, V)	CE$_{max}$ (cd A^{-1}, V)	PE$_{max}$ (lm W^{-1}, V)	λ_{max}	CIE (x, y) at 8 V
B1	PhOXD	3.1	49600, 17.0	26.4, 4.0	55.0, 4.0	48.8, 3.5	472	(0.14, 0.32)
B2	3PyOXD	3.4	36800, 17.5	20.6, 4.0	41.4, 4.0	32.5, 4.0	472	(0.13, 0.32)
B3	4PyOXD	3.1	18900, 16.5	4.7, 4.0	9.4, 4.0	8.7, 3.5	472	(0.14, 0.31)
G1	PhOXD	2.5	162000, 14.0	26.3, 3.0	101.7, 3.0	106.4, 3.0	516	(0.29, 0.64)
G2	3PyOXD	2.6	146000, 16.5	19.5, 5.0	75.9, 5.0	52.5, 4.0	516	(0.29, 0.64)
G3	4PyOXD	3.0	171000, 16.0	17.2, 5.5	67.3, 5.5	41.2, 4.5	514	(0.29, 0.64)
R1	PhOXD	2.7	50300, 15.5	26.6, 4.0	33.8, 4.0	29.4, 3.5	622	(0.67, 0.33)
R2	3PyOXD	2.8	54800, 16.0	26.6, 5.0	33.5, 5.0	23.9, 4.0	620	(0.67, 0.33)
R3	4PyOXD	2.5	65900, 15.0	23.8, 3.5	32.6, 3.5	29.9, 3.0	618	(0.66, 0.34)

[a] L_{max}, maximal luminance; EQE$_{max}$, maximal external quantum efficiency; CE$_{max}$, maximal current efficiency; PE$_{max}$, maximal power efficiency; λ_{max}, wavelength of the EL spectrum at maximal intensity at 8 V. [b] V_d, driving voltage at a brightness of 1 cd m^{-2}.

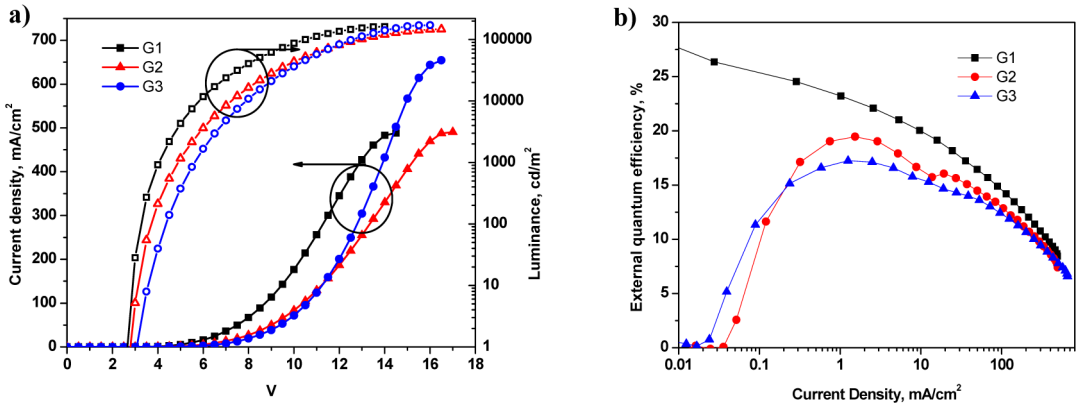

Figure 5. (a) Current density and luminance vs applied voltage. (b) External quantum efficiency vs current density of devices G1−G3. Device structures: ITO/NPB (20 nm)/TCTA (10 nm)/BCPO: Ir(ppy)$_3$ (8%) (30 nm)/PhOXD or 3PyOXD or 4PyOXD (40 nm)/LiF (1 nm)/Al (100 nm).

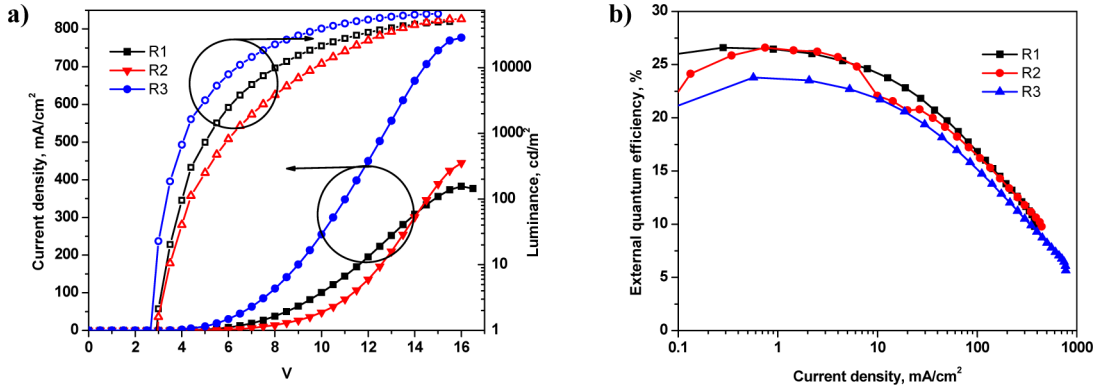

Figure 6. (a) Current density and luminance vs applied voltage. (b) External quantum efficiency vs current density of devices R1−R3. Device structure: ITO/NPB (25 nm)/TCTA (10 nm)/CzPPQ: dopant (4%) (30 nm)/PhOXD or 3PyOXD or 4PyOXD (50 nm)/LiF (1 nm)/Al (100 nm).

8% Ir(ppy)$_3$ as the dopant exhibits a very low turn-on voltage of 2.5 V and a maximal external quantum efficiency, current efficiency, power efficiency, and luminance of 26.3%, 101.7 cd A^{-1}, 106.4 lm W^{-1}, and 162000 cd m^{-2} (14 V), respectively, with CIE values of (0.29, 0.64) (Figure S9 of the Supporting Information). The EQE and current efficiency versus luminance of device G1 is displayed in Figure S10 of the Supporting Information. Similar to blue device B1, G1 also exhibits low-efficiency roll-off and high brightness compared with the devices using the conventional ETL material.[32] At practical brightness levels of 100 and 1000 cd m^{-2}, the EQEs of device G1 still retain at high values of 25.3 and 23.3%, respectively. Devices G2 and G3 exhibit an efficiency lower than that of device G1. However, device G3 displays a very high brightness (171300 cd m^{-2}) compared with that of G1. These results indicate that PhOXD exhibits the highest efficiency, presumably because of the effective electron−hole recombination within the EML compared with those of 3PyOXD and 4PyOXD. 4PyOXD exhibits faster electron mobility, which likely helps the achievement of high brightness and current density (device G3).

The outstanding performance of these *m*-terphenyl oxadiazole compounds as electron-transport materials for blue and green phosphorescence OLEDs inspired us to utilize these

DOI: 10.1021/acsami.5b01872
ACS Appl. Mater. Interfaces 2015, 7, 10466−10474

compounds as electron-transport materials for red phosphorescent OLEDs. Three red devices, R1−R3, using $Ir(piq)_2(acac)$ as the dopant emitter, CzPPQ as the host, and PhOXD, 3PyOXD, and 4PyOXD, respectively, as the ETL material were fabricated. The device structure consists of the following layers: ITO/NPB (25 nm)/TCTA (10 nm)/CzPPQ: $Ir(piq)_2(acac)$ (4%, 30 nm)/ETL (50 nm)/LiF (1 nm)/Al (100 nm), where CzPPQ is 9-(4-(4-phenylquinolin-2-yl)phenyl)-9*H*-carbazole and is the host.[49] Here, 50 nm of ETL is used instead of 40 nm because CzPPQ likely has high electron mobility compared to that of BCPO, and thus, to adjust the recombination in EML, the thickness of ETL is increased. The *I*−*V*−*L* curves and the EQEs versus current density of these three devices are displayed in Figure 6, and the data are summarized in Table 2. Device R1 exhibits a low turn-on voltage of 2.7 V with maximal external quantum efficiency, current efficiency, and power efficiency of 26.6%, 33.8 cd A^{-1}, and 29.4 lm W^{-1}, respectively. These efficiencies are much higher than those of the previously reported $Ir(piq)_2(acac)$-based device using conventional BCP +Alq_3 as the EBL and ETL (EQE of 14.6% and power efficiency of 10.3 lm W^{-1}).[50−52] Device R2 with 3PyOXD as the ETL material exhibits efficiencies very similar to those of R1 except that the maximal power efficiency is only 23.9 lm W^{-1}. Device R3 exhibits a maximal external quantum efficiency of 23.8%, which is approximately 3% lower than the values for R1 and R2. However, the driving voltage (2.5 V) is lower than the corresponding values of devices R1 and R2, and the power efficiency (29.9 lm W^{-1}) and maximal brightness (65900 cd m^{-2}) are higher than the corresponding values of devices R1 and R2. The higher electron mobility and T_g of 4PyOXD compared with those of the other two ETL materials, PhOXD and 3PyOXD, plausibly account for the observed different performance of device R3. Overall, devices R1−R3 exhibit very high brightness and low-turn on voltage because of the high electron mobility of the oxadiazole derivatives. The EQEs and current efficiencies versus luminance and electroluminescent spectra of these devices are shown in Figures S11 and S12 of the Supporting Information. At practical brightnesses of 100 and 1000 cd m^{-2}, the external quantum efficiency of R1 remains at 25.2 and 24%, respectively. These values are much higher than that for the previously reported $Ir(piq)_2(acac)$-based red phosphorescent OLED.[8] Notably, all three compounds can act as eminent electron-transport materials for red phosphorescent OLEDs because PhOXD, 3PyOXD, and 4PyOXD exhibit E_T values higher than those of the host (CzPPQ) and dopant [$Ir(piq)_2acac$], which implies that devices R1−R3 can achieve improved exciton confinement within the EML and reduce the level of triplet exciton quenching in the EML/ETL interface.

To compare the device performances with those of conventional electron-transporting materials, devices B, G, and R were fabricated using OXD-7 as an ETM, and results are listed in Table S1 of the Supporting Information. Devices B, G, and R were fabricated with similar device structures of blue, green, and red, respectively. The result suggests that our newly developed electron-transporting materials show performances for all colors much improved versus those of the conventional ETM. These oxadiazole-based blue, green, and red devices exhibited very low turn-on voltages (3.2 V for blue and 2.5 V for green and red) with excellent external quantum efficiencies, luminances, and current and power efficiencies. Note that PhOXD can be used as a common ETM for all three basic color devices and the efficiencies are among the best known to date.[13,40] On the other hand, 3PyOXD and 4PyOXD can be used as ETMs for green and red devices. To the best of our knowledge, there is no report using a common electron-transporting material to achieve enhanced efficiency for blue, green, and red phosphorescent devices. The overall results suggest that the triplet energy gap, optimal HOMO, LUMO energy level, and electron mobility are very important for the creation of efficient OLEDs.

CONCLUSION

Oxadiazole-based PhOXD, 3PyOXD, and 4PyOXD were synthesized with good yields, and these molecules exhibit high electron mobility, high T_g, and high triplet energy gaps. PhOXD can be used as a universal electron-transport material for blue, green, and red phosphorescent organic light-emitting devices with very high external quantum efficiencies of >26%, which is much higher than that of conventional ET materials. Moreover, these devices exhibit small roll-off even at higher current densities. Selecting an appropriate triplet energy and HOMO and LUMO levels of ETM is very important for a high-performance device. These finding will assist in the new molecular design of ETLs for the further improvement of phosphorescent OLEDs.

ASSOCIATED CONTENT

Supporting Information

Synthesis procedure and chareterization data, CV, DSC, and TGA, electroluminance spectra, external quantum efficiency vs luminance, and current efficiency vs current density. The Supporting Information is available free of charge on the ACS Publications website at DOI: 10.1021/acsami.5b01872.

AUTHOR INFORMATION

Corresponding Author

*E-mail: chcheng@mx.nthu.edu.tw.

Notes

The authors declare no competing financial interest.

ACKNOWLEDGMENTS

We thank the Ministry of Science and Technology of the Republic of China (MOST 103-2633-M-007-001) for support of this research.

REFERENCES

(1) Tang, C. W.; Van Slyke, S. A. Organic Electroluminescent Diodes. *Appl. Phys. Lett.* **1987**, *51*, 913−915.

(2) Xiao, L.; Chen, Z.; Qu, B.; Luo, J.; Kong, S.; Gong, Q.; Kido, J. Recent Progresses on Materials for Electrophosphorescent Organic Light-Emitting Devices. *Adv. Mater. (Weinheim, Ger.)* **2011**, *23*, 926−952.

(3) Shen, Z.; Burrows, P. B.; Bulovic, V.; Forrest, S. R.; Thompson, M. E. Three-Color, Tunable, Organic Light-Emitting Devices. *Science* **1996**, *276*, 2009−2011.

(4) Hung, W.-Y.; Fang, G.-C.; Chang, Y.-C.; Kuo, T.-Y.; Chou, P.-T.; Lin, S.-W.; Wong, K.-T. Highly Efficient Bilayer Interface Exciplex for Yellow Organic Light Emitting Diode. *ACS Appl. Mater. Interfaces* **2013**, *5*, 6826−6831.

(5) Chou, H.-H.; Cheng, C.-H. A Highly Efficient Universal Bipolar Host for Blue, Green, and Red Phosphorescent OLEDs. *Adv. Mater. (Weinheim, Ger.)* **2010**, *22*, 2468−2471.

(6) Ichikawa, M.; Kawaguchi, T.; Kobayashi, K.; Miki, T.; Furukawa, K.; Koyama, T.; Taniguchi, Y. Bipyridyl Oxadiazoles as Efficient and Durable Electron-Transporting and Hole-Blocking Molecular Materials. *J. Mater. Chem.* **2006**, *16*, 221−225.

DOI: 10.1021/acsami.5b01872
ACS Appl. Mater. Interfaces 2015, 7, 10466−10474

(7) Chou, H. H.; Chen, Y. H.; Hsu, H. P.; Chang, W. H.; Chen, Y. H.; Cheng, C. H. Synthesis of Diimidazolylstilbenes as n-Type Blue Fluorophores; Alternative Dopant Materials for Highly Efficient Electroluminescent Devices. *Adv. Mater. (Weinheim, Ger.)* **2012**, *24*, 5867−5871.
(8) Fan, C. C.; Sun, P. P.; Su, T. H.; Cheng, C. H. Host and Dopant Materials for Idealized Deep Red Organic Electrophosphorescence Devices. *Adv. Mater. (Weinheim, Ger.)* **2011**, *23*, 2981−2985.
(9) Chen, C.-H.; Wu, F.-I.; Tsai, Y.-Y.; Cheng, C.-H. Platinum Phosphors Containing an Aryl-modified β-Diketonate: Unusual Effect of Molecular Packing on Photo- and Electroluminescence. *Adv. Funct. Mater.* **2011**, *21*, 3150−3158.
(10) Poloek, A.; Chen, C.-T.; Chen, C.-T. High Performance Hybrid White and Multi-Colour Electroluminescence from a New Host Material for Heteroleptic Naphthyridinolate Platinum Complex Dopant. *J. Mater. Chem. C* **2014**, *2*, 1376−1380.
(11) Baldo, M. A.; O'Brien, D. F.; You, Y.; Shoustikov, A.; Sibley, S.; Thompson, M. E.; Forrest, S. R. Highly Efficient Phosphorescent Emission from Organic Electroluminescent Devices. *Nature* **1998**, *395*, 151−154.
(12) Baldo, M. A.; Thompson, M. E.; Forrest, S. R. High-efficiency Fluorescent Organic Light-Emitting Devices Using a Phosphorescent Sensitizer. *Nature* **2000**, *403*, 750−753.
(13) Chen, C.-H.; Wu, F.-I.; Tsai, Y.-Y.; Cheng, C.-H. Platinum Phosphors Containing an Aryl-modified β- Diketonate: Unusual Effect of Molecular Packing on Photo- and Electroluminescence. *Adv. Funct. Mater.* **2011**, *21*, 3150−3158.
(14) Liu, D.; Ren, H.; Deng, L.; Zhang, T. Synthesis and Electrophosphorescence of Iridium Complexes Containing Benzothiazole-Based Ligands. *ACS Appl. Mater. Interfaces* **2013**, *5*, 4937−4944.
(15) Lu, K. Y.; Chou, H. H.; Hsieh, C. H.; Yang, Y. H.; Tsai, H. R.; Tsai, H. Y.; Hsu, L. C.; Chen, C. Y.; Chen, I. C.; Cheng, C. H. Wide-Range Color Tuning of Iridium Biscarbene Complexes from Blue to Red by Different N^N Ligands: An Alternative Route for Adjusting the Emission Colors. *Adv. Mater. (Weinheim, Ger.)* **2011**, *23*, 4933−4937.
(16) Du, B.-S.; Liao, J.-L.; Huang, M.-H.; Lin, C.-H.; Lin, H.-W.; Chi, Y.; Fan, G.-L.; Wong, K.-T.; Lee, G.-H.; Chou, P.-T. Os(II) Based Green to Red Phosphors: A Great Prospect for Solution-Processed, Highly Efficient Organic Light-Emitting Diodes. *Adv. Funct. Mater.* **2012**, *22*, 3491−3499.
(17) Gong, S.; Chen, Y.; Luo, J.; Yang, C.; Zhong, C.; Qin, J.; Ma, D. Bipolar Tetraarylsilanes as Universal Hosts for Blue, Green, Orange, and White Electrophosphorescence with High Efficiency and Low Efficiency Roll-Off. *Adv. Funct. Mater.* **2011**, *21*, 1168−1178.
(18) Gong, S.; Chen, Y.; Yang, C.; Zhong, C.; Qin, J.; Ma, D. De Novo Design of Silicon-Bridged Molecule Towards a Bipolar Host: All-Phosphor White Organic Light-Emitting Devices Exhibiting High Efficiency and Low Efficiency Roll-Off. *Adv. Mater. (Weinheim, Ger.)* **2010**, *22*, 5370−5373.
(19) Gong, S.; Fu, Q.; Wang, Q.; Yang, C.; Zhong, C.; Qin, J.; Ma, D. Highly Efficient Deep-Blue Electrophosphorescence Enabled by Solution-Processed Bipolar Tetraarylsilane Host with Both a High Triplet Energy and a High-Lying HOMO Level. *Adv. Mater. (Weinheim, Ger.)* **2011**, *23*, 4956−4959.
(20) Chopra, N.; Lee, J.; Zheng, Y.; Eom, S.-H.; Xue, J.; So, F. High Efficiency Blue Phosphorescent Organic Light-Emitting Device. *Appl. Phys. Lett.* **2008**, *93*, 143307−143309.
(21) Strohriegl, P.; Grazulevicius, J. V. Charge-Transporting Molecular Glasses. *Adv. Mater. (Weinheim, Ger.)* **2002**, *14*, 1439−1452.
(22) Tomkeviciene, A.; Grazulevicius, J. V.; Kazlauskas, K.; Gruodis, A.; Jursenas, S.; Ke, T.-H.; Wu, C.-C. Impact of Linking Topology on the Properties of Carbazole Trimers and Dimers. *J. Phys. Chem. C* **2011**, *115*, 4887−4897.
(23) Li, Y.; Fung, M. K.; Xie, Z.; Lee, S. T.; Hung, L.-S.; Shi, J.; Li, Y. Q. An Efficient Pure Blue Organic Light-Emitting Device with Low Driving Voltages. *Adv. Mater. (Weinheim, Ger.)* **2002**, *14*, 1317−1321.
(24) Antoniadis, H.; Abkowitz, M. A.; Hsieh, B. R. Carrier Deep-Trapping Mobility-Lifetime Products in Poly(*p*-Phenylene Vinylene). *Appl. Phys. Lett.* **1994**, *65*, 2030−2032.
(25) Yoo, S.-J.; Yun, H.-J.; Kang, I.; Thangaraju, K.; Kwon, S.-K.; Kim, Y.-H. A New Electron Transporting Material for Effective Hole-Blocking and Improved Charge Balance in Highly Efficient Phosphorescent Organic Light Emitting Diodes. *J. Mater. Chem. C* **2013**, *1*, 2217−2223.
(26) Sun, Y.; Giebink, N. C.; Kanno, H.; Ma, B.; Thompson, M. E.; Forrest, S. R. Management of Singlet and Triplet Excitons for Efficient White Organic Light-Emitting Devices. *Nature* **2006**, *440*, 908−912.
(27) Ruden, A. L. V.; Cosimbescu, L.; Polikarpov, E.; Koech, P. K.; Swensen, J. S.; Wang, L.; Darsell, J. T.; Padmaperuma, A. B. Phosphine Oxide Based Electron Transporting and Hole Blocking Materials for Blue Electrophosphorescent Organic Light Emitting Devices. *Chem. Mater.* **2010**, *22*, 5678−5686.
(28) Sun, C.; Hudson, Z. M.; Helander, M. G.; Lu, Z.-H.; Wang, S. A Polyboryl-Functionalized Triazine as an Electron Transport Material for OLEDs. *Organometallics* **2011**, *30*, 5552−5555.
(29) Jeon, S. O.; Yook, K. S.; Joo, C. W.; Lee, J. Y. A phosphine oxide derivative as a universal electron transport material for organic light-emitting diodes. *J. Mater. Chem.* **2009**, *19*, 5940−5944.
(30) Wu, C.-A.; Chou, H.-H.; Shih, C.-H.; Wu, F.-I.; Cheng, C.-H.; Huang, H.-L.; Chao, T.-C.; Tseng, M.-R. Synthesis and Physical Properties of Meta-Terphenyloxadiazole Derivatives and Their Application as Electron Transporting Materials for Blue Phosphorescent and Fluorescent Devices. *J. Mater. Chem.* **2012**, *22*, 17792−17799.
(31) Padmaperuma, A. B.; Sapochak, L. S.; Burrows, P. E. New Charge Transporting Host Material for Short Wavelength Organic Electrophosphorescence: 2,7-Bis(diphenylphosphine oxide)-9,9-dimethylfluorene. *Chem. Mater.* **2006**, *18*, 2389−2396.
(32) Su, S.-J.; Chiba, T.; Takeda, T.; Kido, J. Pyridine-Containing Triphenylbenzene Derivatives with High Electron Mobility for Highly Efficient Phosphorescent OLEDs. *Adv. Mater. (Weinheim, Ger.)* **2008**, *20*, 2125−2130.
(33) Su, S.-J.; Sasabe, H.; Takeda, T.; Kido, J. Pyridine-Containing Bipolar Host Materials for Highly Efficient Blue Phosphorescent OLEDs. *Chem. Mater.* **2008**, *20*, 1691−1693.
(34) Su, S.-J.; Sasabe, H.; Pu, Y.-J.; Nakayama, K.-i.; Kido, J. Tuning Energy Levels of Electron-Transport Materials by Nitrogen Orientation for Electrophosphorescent Devices with an 'Ideal' Operating Voltage. *Adv. Mater. (Weinheim, Ger.)* **2010**, *22*, 3311−3316.
(35) Su, S.-J.; Takahashi, Y.; Chiba, T.; Takeda, T.; Kido, J. Structure−Property Relationship of Pyridine-Containing Triphenyl Benzene Electron-Transport Materials for Highly Efficient Blue Phosphorescent OLEDs. *Adv. Funct. Mater.* **2009**, *19*, 1260−1267.
(36) Ye, H.; Chen, D.; Liu, M.; Su, S.-J.; Wang, Y.-F.; Lo, C.-C.; Lien, A.; Kido, J. Pyridine-Containing Electron-Transport Materials for Highly Efficient Blue Phosphorescent OLEDs with Ultralow Operating Voltage and Reduced Efficiency Roll-Off. *Adv. Funct. Mater.* **2014**, *24*, 3268−3275.
(37) Li, X.-L.; Ye, H.; Chen, D.-C.; Liu, K.-K.; Xie, G.-Z.; Wang, Y.-F.; Lo, C.-C.; Lien, A.; Peng, J.; Cao, Y.; Su, S.-J. Triazole and Pyridine Hybrid Molecules as Electron-Transport Materials for Highly Efficient Green Phosphorescent Organic Light-Emitting Diodes. *Isr. J. Chem.* **2014**, *54*, 971−978.
(38) Lee, J.-H.; Wang, P.-S.; Park, H.-D.; Wu, C.-I.; Kim, J.-J. A High Performance Inverted Organic Light Emitting Diode using an Electron Transporting Material with Low Energy Barrier for Electron Injection. *Org. Electron.* **2011**, *12*, 1763−1767.
(39) Jeon, S. O.; Earmme, T.; Jenekhe, S. A. New Sulfone-Based Electron-Transport Materials with High Triplet Energy for Highly Efficient Blue Phosphorescent Organic Light-Emitting Diodes. *J. Mater. Chem. C* **2014**, *2*, 10129−10137.
(40) Shih, C.-H.; Rajamalli, P.; Wu, C.-A.; Chiu, M.-J.; Chu, L.-K.; Cheng, C.-H. A High Triplet Energy, High Thermal Stability Oxadiazole Derivative as the Electron Transporter for Highly Efficient Red, Green and Blue Phosphorescent OLEDs. *J. Mater. Chem. C* **2015**, *3*, 1491−1496.

DOI: 10.1021/acsami.5b01872
ACS Appl. Mater. Interfaces 2015, 7, 10466−10474

(41) Yang, C.-C.; Hsu, C.-J.; Chou, P.-T.; Cheng, H. C.; Su, Y. O.; Leung, M.-k. Excited State Luminescence of Multi-(5-phenyl-1,3,4-oxadiazo-2-yl)benzenes in an Electron-Donating Matrix: Exciplex or Electroplex? *J. Phys. Chem. B* **2010**, *114*, 756−768.
(42) Yasuda, T.; Yamaguchi, Y.; Zou, D.-C.; Tsutsui, T. Carrier Mobilities in Organic Electron Transport Materials Determined from Space Charge Limited Current. *Jpn. J. Appl. Phys.* **2002**, *41*, 5626−5629.
(43) Lee, C. W.; Lee, J. Y. Structure−Property Relationship of Pyridoindole-Type Host Materials for High-Efficiency Blue Phosphorescent Organic Light-Emitting Diodes. *Chem. Mater.* **2014**, *26*, 1616−1621.
(44) Xiao, L.; Qi, B.; Xing, X.; Zheng, L.; Kong, S.; Chen, Z.; Qu, B.; Zhang, L.; Ji, Z.; Gong, Q. A Weak Electron Transporting Material with High Triplet Energy and Thermal Stability via a Super Twisted Structure for High Efficient Blue Electrophosphorescent Devices. *J. Mater. Chem.* **2011**, *21*, 19058−19062.
(45) Rhee, S. H.; Nam, K. b.; Kim, C. S.; Song, M.; Cho, W.; Jin, S.-H.; Ryu, S. Y. Effect of Electron Mobility of the Electron Transport Layer on Fluorescent Organic Light-Emitting Diodes. *ECS Solid State Lett.* **2014**, *3*, R19−R22.
(46) Baldo, M. A.; Adachi, C.; Forrest, S. R. Transient Analysis of Organic Electrophosphorescence. II. Transient Analysis of Triplet-Triplet Annihilation. *Phys. Rev. B* **2000**, *62*, 10967−10977.
(47) Xiao, L.; Su, S.-J.; Agata, Y.; Lan, H.; Kido, J. Nearly 100% Internal Quantum Efficiency in an Organic Blue-Light Electrophosphorescent Device Using a Weak Electron Transporting Material with a Wide Energy Gap. *Adv. Mater. (Weinheim, Ger.)* **2009**, *21*, 1271−1274.
(48) Lyu, Y.-Y.; Kwak, J.; Jeon, W. S.; Byun, Y.; Lee, H. S.; Kim, D.; Lee, C.; Char, K. Highly Efficient Red Phosphorescent OLEDs based on Non-Conjugated Silicon-Cored Spirobifluorene Derivative Doped with Ir-Complexes. *Adv. Funct. Mater.* **2009**, *19*, 420−427.
(49) Chen, C.-H.; Hsu, L.-C.; Rajamalli, P.; Chang, Y.-W.; Wu, F.-I.; Liao, C.-Y.; Chiu, M.-J.; Chou, P.-Y.; Huang, M.-J.; Chu, L.-K.; Cheng, C.-H. Highly Efficient Orange and Deep-Red Organic Light Emitting Diodes with Long Operational Lifetimes using Carbazole−Quinoline based Bipolar Host Materials. *J. Mater. Chem. C* **2014**, *2*, 6183−6191.
(50) Ikai, M.; Tokito, S.; Sakamoto, Y.; Suzuki, T.; Taga, Y. Highly Efficient Phosphorescence from Organic Light-Emitting Devices with an Exciton-Block Layer. *Appl. Phys. Lett.* **2001**, *79*, 156−158.
(51) Adachi, C.; Baldo, M. A.; Forrest, S. R.; Thompson, M. E. High-Efficiency Organic Electrophosphorescent Devices with Tris(2-Phenylpyridine)Iridium Doped Into Electron-Transporting Materials. *Appl. Phys. Lett.* **2000**, *77*, 904−906.
(52) Chu, T.-Y.; Wu, Y.-S.; Chen, J.-F.; Chen, C. H. Characterization of Electronic Structure of Aluminum(III) Bis(2-Methyl-8-Quninolinato)-4-Phenylphenolate (BAlq) for Phosphorescent Organic Light Emitting Devices. *Chem. Phys. Lett.* **2005**, *404*, 121−125.

DOI: 10.1021/acsami.5b01872
ACS Appl. Mater. Interfaces 2015, 7, 10466−10474